DOI: 10.1002/chem.200501095

π-Conjugated Chelating Polymers with Charged Iridium Complexes in the Backbones: Synthesis, Characterization, Energy Transfer, and Electrochemical Properties

Shu-Juan Liu, Qiang Zhao, Run-Feng Chen, Yun Deng, Qu-Li Fan,* Fu-You Li, Lian-Hui Wang, Chun-Hui Huang, and Wei Huang*[a]

Abstract: A series of π-conjugated chelating polymers with charged iridium (Ir) complexes in the backbones were synthesized by a Suzuki polycondensation reaction, leading to homogeneous polymeric materials that phosphoresce red light. The fluorene and bipyridine (bpy) segments were used as polymer backbones. 5,5′-Dibromobipyridine served as a ligand to form a charged iridium complex monomer with 1-(9′9-dioctylfluorene-2-yl)isoquinoline (Fiq) as the cyclometalated ligand. Chemical and photophysical characterization confirmed that Ir complexes were incorporated into the backbones as one of the repeat units by means of the 5,5′-dibromobipyridine ligand. Chelating polymers showed almost complete energy transfer from the host fluorene segments to the guest Ir complexes in the solid state when the feed ratio was 2 mol%. In the films of the corresponding blend system, however, energy transfer was not complete even when the content of Ir complexes was as high as 16 mol%. Both intra- and intermolecular energy-transfer processes existed in this host–guest system, and the intramolecular energy transfer was a more efficient process. All chelating polymers displayed good thermal stability, redox reversibility, and film formation. These chelating polymers also showed more efficient energy transfer than the corresponding blended system and the mechanism of incorporation of the charged Ir complexes into the π-conjugated polymer backbones efficiently avoided the intrinsic problems associated with the blend system, thus offering promise in optoelectronic applications.

Keywords: chelates · host–guest systems · iridium · luminescence · polymers

Introduction

In the past few years, organic phosphorescent light-emitting materials have attracted increasing attention owing to their good performance and potential applications in light-emitting electrochemical cells (LECs) and full-color flat-panel displays.[1] Nearly 100% internal quantum efficiency can be achieved because of the full utilization of singlet and triplet excitons owing to the strong spin-orbital mixing of heavy-metal ions in the complexes.[2] Among phosphorescent heavy-metal complexes, iridium complexes have been considered as one of the best phosphorescent-material candidates because they show intense phosphorescence at room temperature and significantly shorter phosphor lifetime compared with other heavy-metal complexes, which is crucial for the performance of phosphorescent materials. Moreover, the emission color can be tuned easily over the entire visible region by modifying the structure of the ligand.[3] For display-related applications, Ir complexes were doped into host materials to reduce triplet–triplet (T–T) annihilation and concentration quenching, thus improving performance of the devices.[4] Neutral complexes have been of most interest probably due to their compatibility with hydrophobic matrices. Efficient energy transfer can be expected in the blend system of polymer and Ir complex. Carbazole (Cz) segment-based polymers and poly(9,9-alkylfluorene) (PF)[5] are often used as hosts, and the corresponding highly efficient devices emitting from blue to red in the visible spectrum have been reported.

Although devices in which phosphorescent dyes are doped into polymeric hosts have successfully produced highly efficient polymer light-emitting diodes (PLEDs),

[a] S.-J. Liu, Q. Zhao, R.-F. Chen, Y. Deng, Dr. Q.-L. Fan, Dr. F.-Y. Li, Prof. L.-H. Wang, Prof. C.-H. Huang, Prof. W. Huang
Institute of Advanced Materials (IAM)
Fudan University, 220 Handan Road, Shanghai 200433 (China)
Fax: (+86) 21-6565-5123
E-mail: qlfan@fudan.edu.cn
wei-huang@fudan.edu.cn

these devices may undergo phase separation, leading to fast reduction of efficiency with increasing current density. An efficient solution to this problem is to introduce phosphorescent dye into the polymer chain by means of a chemical bond.[6] Chen and co-workers[7] synthesized phosphorescent conjugated polymers based on a poly(fluorene) backbone with Ir complex pendants attached to the C-9 position of the fluorine group. Sandee and co-workers[8] reported chelating polymers with the complexes in the main chains. Other polymers with Ir complexes in the conjugated polymer chains were obtained by using similar approaches.[5d,9] Nonconjugated polymers with Ir complex pendants attached have also been reported.[10]

However, compared with neutral complexes, charged Ir complexes have many features that may make them one of the best candidates for lighting and display applications according to reports of recent studies.[11] Inert metal electrodes that are resistant to oxidation in air can be used in devices containing charged Ir complexes and the power consumption of these devices is low. We can expect further improvement of the stability of these devices due to the excellent redox stability of charged Ir complexes. They also possess charge-transfer properties. But the compatibility between charged Ir complex guest and hydrophobic polymer host is still a problem that could hinder the development of their applications. Therefore it is necessary to introduce charged Ir complexes into polymer main chains or side chains by using a chemical bond. The matrices can be conjugated or nonconjugated polymers. The synthesis and photophysical properties of novel iridium complexes that have been functionalized by monoterpyridine-PEG, poly(ethylene oxide) (PEO), and poly(styrene) (PS) have been reported.[12] However, there was no energy and charge transfer in these systems because the main chains were not conjugated and the complex was only on the end group. It would be interesting to investigate π-conjugated chelating polymers with charged Ir complexes as a repeated unit incorporated into the main chain. The conjugated segment plays two roles as polymer ligand and host for the energy transfer system.

Herein, we report the successful synthesis of a series of new red-light-emitting polymers with charged iridium complexes in the backbones, in which the phosphorescent chromophores were molecularly dispersed within the composite material. Poly(9,9-dioctylfluorene) (PFO) was selected as host because of the high fluorescence, charge transport properties, and good chemical and thermal stability. To the best of our knowledge, this is the first report of red-phosphorescent π-conjugated polymers with charged Ir complexes in the backbones by copolymerization of a fluorene unit and a charged Ir complex unit. The synthesis and characterization are described together with detailed studies of the photophysical properties, energy transfer in the host–guest system, and electrochemical properties. Preliminary results indicate that these materials are promising in optoelectronic applications.

Results and Discussion

Synthesis of the complexes and copolymers: The synthesis route leading to the Ir complexes is shown in Scheme 1. The Ir complexes were synthesized from corresponding bipyridine (bpy) and iridium–chloride-bridged dimers. The copolymers from fluorene and iridium-complex-chelated 5,5′-dibromo-2,2′-bipyridine were prepared by using a Suzuki polycondensation as shown in Scheme 2. The feed ratios of iridium complex in the polycondensation were 0, 0.5, 2, 4, 8, and 16 mol%, and the corresponding polymers were named PFO, PFO-Ir05, PFO-Ir2, PFO-Ir4, PFO-Ir8, and PFO-Ir16, respectively.

Figure 1 shows the ^{1}H NMR spectra of the chelating polymers and the Ir complex monomer. Some resonances due to the Ir complexes in chelating polymers, such as the peaks at $\delta \approx 9.02$, 8.30, 7.10, and 6.80 ppm, could be clearly found in the ^{1}H NMR spectra of chelating polymers when the content of Ir complexes was sufficient. These peaks intensified with the increase in the amount of Ir complexes in the chelating polymers, indicating the successful incorporation of Ir complexes. More importantly, the chelating polymers used in our work showed different photophysical properties from those of the corresponding blend system (discussed below), similar to the experimental phenomena reported on chelating polymers with neutral Ir complexes in the conjugated backbones,[6a] which further demonstrates that the Ir complexes were successfully incorporated into the molecular structure of the polymers. The iridium content in the copolymers was estimated by combining the ^{1}H NMR data with elemental analysis data. The feed ratios of the monomers and actual compositions of the chelating polymers are listed in Table 1. The results showed that the actual content of charged Ir complexes in the chelating polymers was lower than that in the feed ratios. The difference of reaction activity and/or steric hindrance of charged Ir complexes might be responsible for this. The actual charged-Ir-complex content in the copolymers PFO-Ir05 and PFO-Ir2 were not estimated due to the limitations in the accuracy of the elemental analysis and the very low intensity of peaks of iridium complexes in the ^{1}H NMR spectra that were difficult to integrate.[7] The weight-average molecular weights (estimated by gel permeation chromatography (GPC) in THF by using the calibration curve of poly(styrene) standards) of these chelating polymers ranged from 9600 to 20800, with a polydispersity index (PDI) of 1.20–1.81, which is consistent with a Suzuki polycondensation reaction.[13] It was reported previously that nonconjugated polymers with Ir complexes were proved to be stable by using the photo diode-array detector of a GPC system[3e] because the photophysical properties of the outflow were in full agreement with those measured in solutions. Accordingly, for the chelating polymers studied here, the stability was demonstrated by using a similar method and they would not be fragmented during the GPC measurement.

The thermal stability of the chelating polymers in nitrogen gas was evaluated by thermogravimetric analysis (TGA;

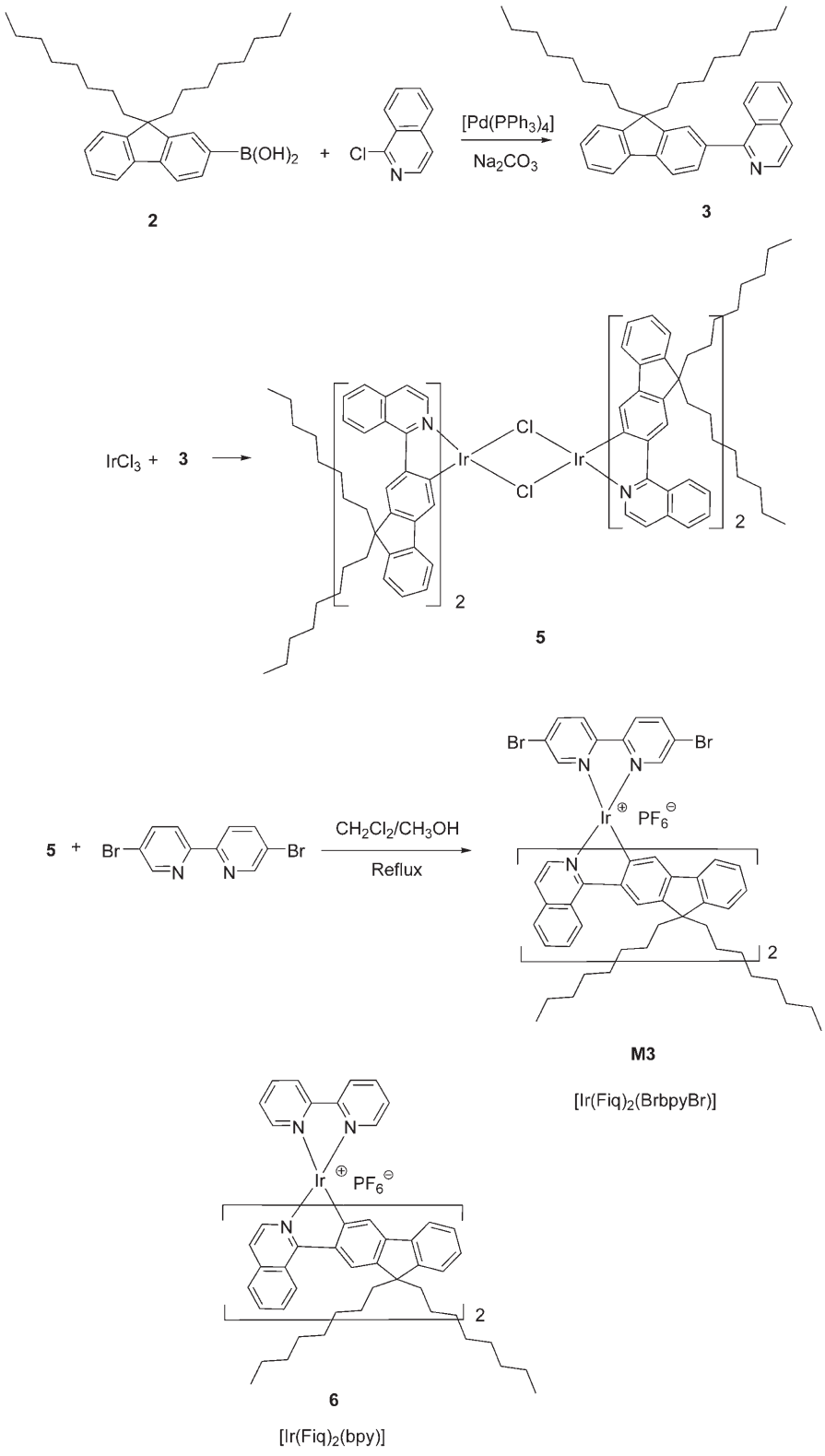

Scheme 1. Synthesis of iridium complexes.

Figure 2). The corresponding data are summarized in Table 2. The decomposition temperatures (T_d) were 414, 383, 398, 340, and 324 °C with a weight loss of 5% for PFO-Ir05, PFO-Ir2, PFO-Ir4, PFO-Ir8, and PFO-Ir16, respectively, indicative of good thermal stability. This may in turn improve the operating lifetime of the EL device.[14] Thermally induced phase-transition behavior of the chelating polymers was also investigated with differential scanning calorimetry (DSC) in a nitrogen atmosphere (Figure 3). The DSC data are also shown in Table 2. Copolymers PFO-Ir16 and PFO-Ir8 showed no phase transition in the heating scan. These chelating polymers showed a much higher glass-transition temperatures (T_g) (ca. 110–116 °C) compared with typical poly(fluorene) (<60 °C).[15] The amorphism and relatively high T_g temperatures are essential for many applications, such as in light-emitting diodes used as emissive materials.[16]

Optical properties: Figure 4 shows the photoluminescence (PL) spectrum of host polymer PFO and the UV/Vis absorption spectrum of [Ir(Fiq)$_2$(bpy)]. The absorption spectrum of [Ir(Fiq)$_2$(bpy)] shows broad bands from 270 to 500 nm, with the most-intense bands at $\lambda < 300$ nm and moderately intense bands at longer wavelengths, which extend far within the visible region. The absorption bands at $\lambda < 300$ nm were mainly due to spin-allowed π–π* ligand-centered (LC) transitions. In particular, on the basis of the literature data,[17] the absorption bands peaking at around 297 nm receive larger contributions from bipyridine-centered transitions. The absorption peaks at around $\lambda > 400$ nm could be assigned to the spin-allowed singlet metal-to-ligand charge-transfer (^{1}MLCT) transitions and the peaks at lowest energy ($\lambda > 450$ nm) were assigned to spin-forbidden triplet metal-to-ligand charge-transfer (^{3}MLCT) transitions owing to the large spin-orbit-coupling induced by

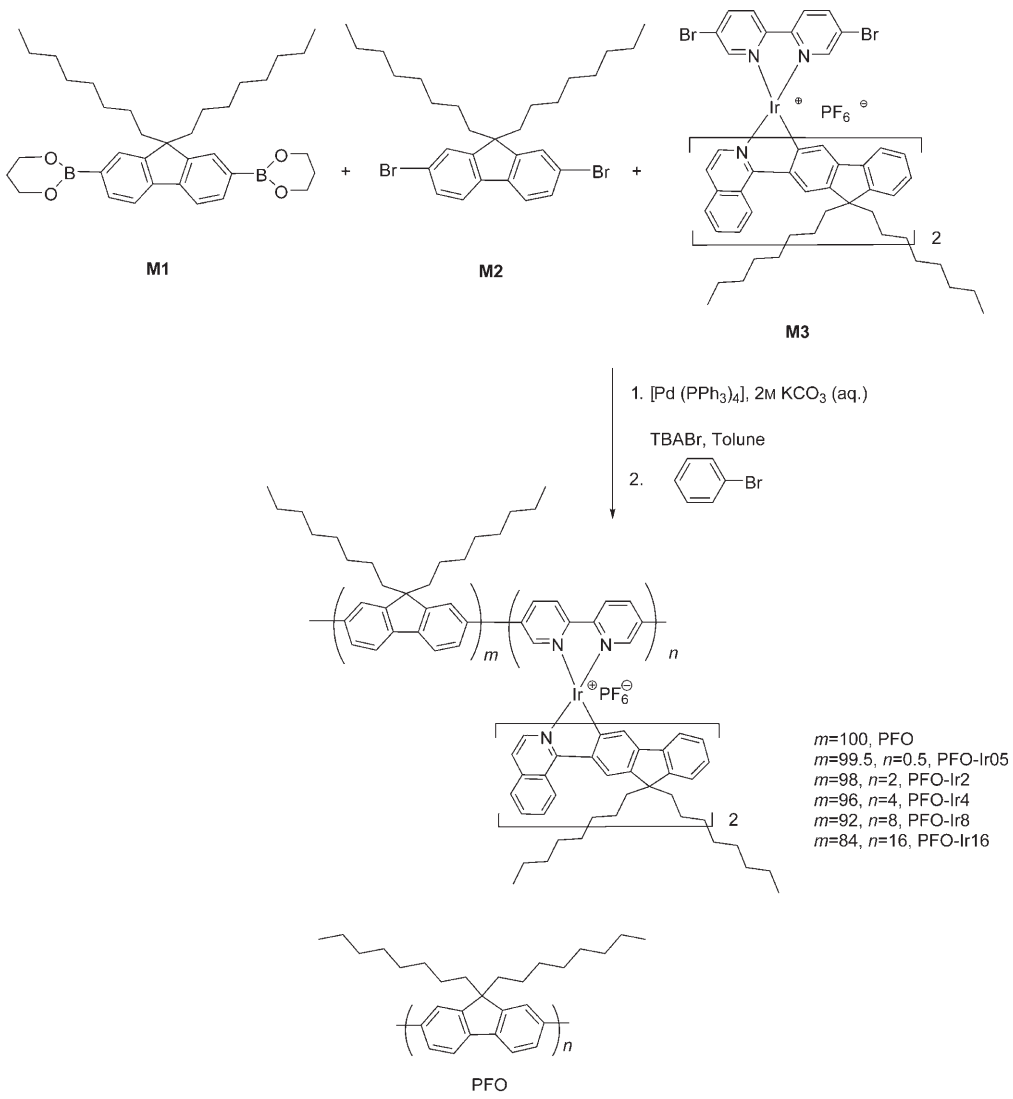

Scheme 2. Synthesis of the polymers.

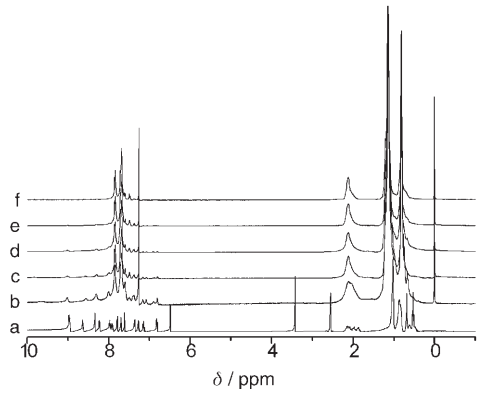

Figure 1. ^{1}H NMR spectra of the chelating polymers and iridium complex monomer. a) [Ir(Fiq)$_2$(BrbpyBr)]; b) PFO-Ir16; c) PFO-Ir8; d) PFO-Ir4; e) PFO-Ir2; f) PFO-Ir05.

Table 1. Molecular weight, polydispersity index, and composition of the polymers.

Polymer			Complex content [mol %]	
	10^{-3} M_w[a]	PDI	feed ratio	in copolymers[b]
PFO	12.1	1.81	–	–
PFO-Ir05	18.8	1.79	0.5	–
PFO-Ir2	20.8	1.70	2	–
PFO-Ir4	23.2	1.64	4	3.6
PFO-Ir8	13.7	1.43	8	5.5
PFO-Ir16	9.6	1.20	16	11

[a] Weight-average molecular weight M_w was estimated by GPC in THF by using a calibration curve of poly(styrene) standards. [b] Estimated from the ^{1}H NMR and elemental analysis data.[7]

the heavy-metal iridium center. It can be seen from Figure 4 that there is good spectral overlap between the PL emission spectrum of the host polymer PFO and the absorption spectrum of the guest Ir complexes. In the Föster mechanism,[18] the dipole–dipole interaction results in efficient transfer of the singlet-excited-state energy from the host to the guest. The efficiency of the Föster energy transfer is dependent on

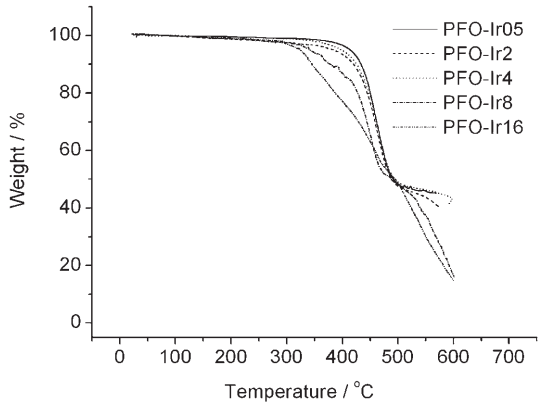

Figure 2. Thermograms of copolymers measured in nitrogen atmosphere.

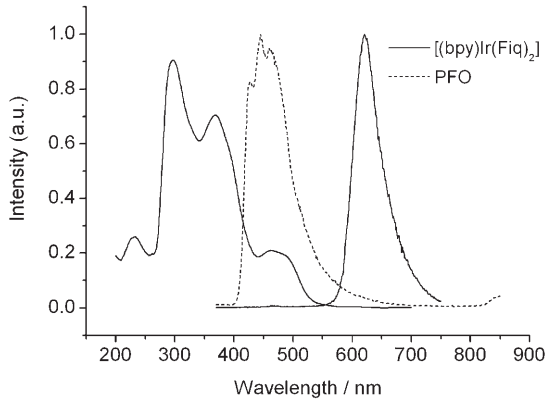

Figure 4. PL spectra of PFO and UV/Vis absorption and PL spectra of the guest Ir complex in a film excited at 325 nm.

Table 2. Physical properties for polymers and $[Ir(Fiq)_2(bpy)]$.

Polymer	λ_{max}[a] [nm]	Φ_{PL}[b] [%]	τ_1[b,c] [ns]	τ_2[b,d] [μs]	T_g [°C]	T_d[e] [°C]
PFO	445	40.1	2.40	–	–	–
PFO-Ir05	624	6.1	1.88	1.51	113	414
PFO-Ir2	625	5.0	1.65	1.20	116	383
PFO-Ir4	628	4.7	–	1.10	116	398
PFO-Ir8	629	3.5	–	1.01	No	341
PFO-Ir16	631	3.1	–	0.52	No	324
$[Ir(Fiq)_2(bpy)]$	321	–	–	–	–	–

[a] Wavelength of maximum of emission, measured at room temperature for film spun from $CHCl_3$. [b] Measured at room temperature for film spun from $CHCl_3$. [c] Monitored at λ of 445 nm. [d] Monitored at peak emission. [e] Temperature of 5% weight loss measured by TGA in nitrogen.

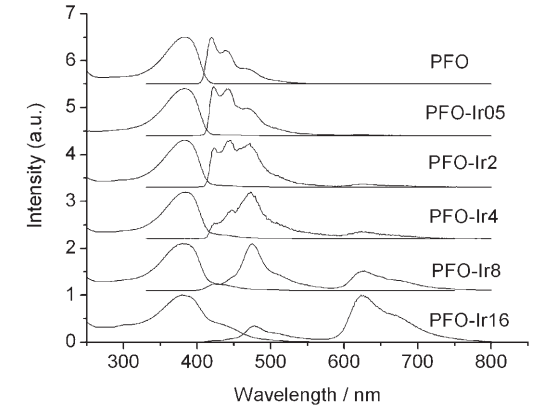

Figure 5. Absorption and PL spectra of polymers in CH_2Cl_2 solution at 2.5×10^{-5} M excited at 325 nm.

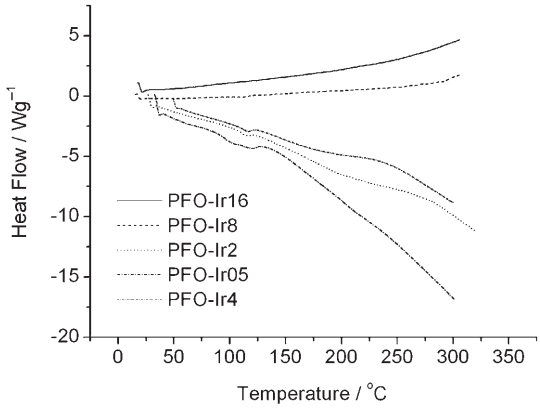

Figure 3. DSC traces of copolymers measured in a nitrogen atmosphere.

the spectral overlap between the host emission spectrum and the guest absorption spectrum.[19] Therefore, the good overlap of the host polymer emission and guest absorption in this host–guest system ensures efficient Föster energy transfer from the host PFO to the guest $[Ir(Fiq)_2(bpy)]$.

Figure 5 shows the UV/Vis absorption and PL spectra of solutions for chelating polymers and PFO. The UV/Vis spectra of the chelating polymers with a low content of Ir complexes were dominated by a single peak with maximum absorbance at around 380 nm (almost the same as that of PFO). A weak absorption peak along with the main absorption peak and extending far within the visible region appeared in the spectrum of PFO-Ir4, and its intensity increased with the increase of charged Ir-complex-unit content in the copolymers. It was attributed to MLCT transitions of the iridium complex. Figure 6 shows the UV/Vis absorption and PL spectra of films for the chelating polymers and PFO, and it was found that the UV/Vis absorption spectra of films for chelating polymers were similar to those in solutions (Figure 6).

Photophysical properties and energy transfer: Figure 7 shows the PL spectra for solutions of different concentrations of polymer PFO-Ir16 in CH_2Cl_2 and for the corresponding blended system with the same content of Ir complexes. For the chelating polymer PFO-Ir16 the emission from the Ir complexes was observed when the concentration was 10^{-7} M, while at the same concentration we could not observe it in the spectra of the corresponding blended system. It is well known that molecules at the low concen-

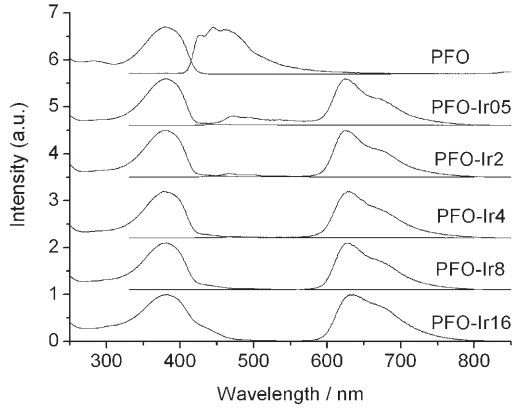

Figure 6. Absorption and PL spectra of films of polymers excited at 325 nm.

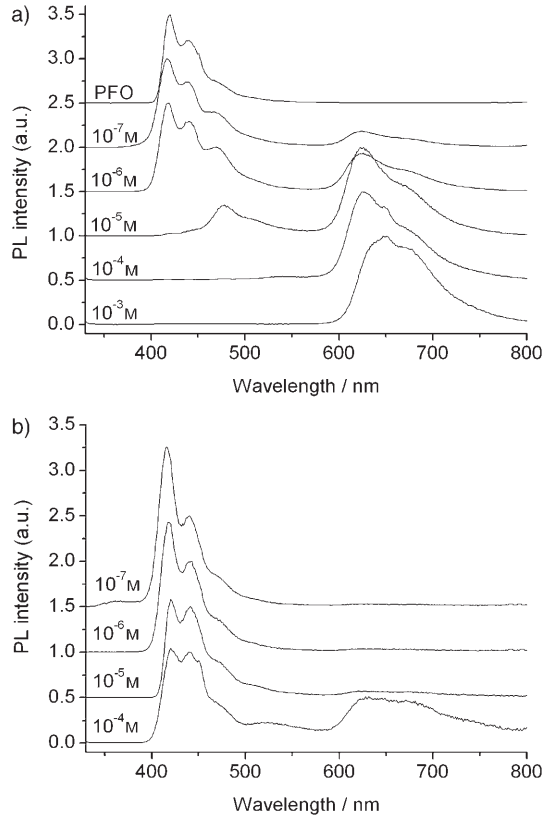

Figure 7. PL spectra of different concentration solutions of copolymer PFO-Ir16 (a) and corresponding blend system (b) in CH_2Cl_2 excited at 325 nm.

tration of 10^{-7} M mainly show characteristics of single molecules because of the long distance between two molecules. In the blended system, their intermolecular energy transfer highly depends on the distance between host and guest. Therefore the intermolecular energy transfer in the blended system was impeded due to the long distance between the host PFO and the guest [Ir(Fiq)$_2$(bpy)][19] at the low concentration of 10^{-7} M and no emission from [Ir(Fiq)$_2$(bpy)] was observed. Likewise, the intermolecular energy transfer of chelating polymers can also be ignored at 10^{-7} M. However, we found that the emission from [Ir(Fiq)$_2$(bpy)] was observable in the PL spectrum of PFO-Ir16 at 10^{-7} M and was attributable to the existence of efficient intramolecular energy transfer of PFO-Ir16 in its dilute solution. This phenomenon showed that intramolecular energy transfer is intrinsic in chelating polymers. In Figure 7a, we also found that the intensity of the blue emission decreased whilst that of the red emission increased with increasing concentration of chelating polymer. This observation showed that energy transfer became more efficient and intermolecular energy transfer started to occur due to the closer distance between host and guest at higher concentration. We also noticed that the blended system showed energy transfer with concentrations up to 10^{-4} M. For PFO-Ir16, however, energy transfer was almost complete at 10^{-5} M, indicating that the energy transfer in the chelating polymers was more efficient than that in the corresponding blended system.

The PL spectra of the chelating polymers in CH_2Cl_2 solutions at 2.5×10^{-5} M are shown in Figure 5. We could only find a strong blue emission band (at around 445 nm) in the spectrum of PFO-Ir05, which was assigned to π–π^* transitions of copolymer backbones without iridium complexes. A weak red emission band (at around 626 nm) assigned to the emission from iridium complexes appeared in the spectrum for PFO-Ir2, and its intensity increased as the content of charged Ir complex increased, indicating the energy transfer process of this system. In the spectrum of PFO-Ir16, the red emission band (at around 623 nm) was dominant. The observations suggest that the energy transfer becomes efficient with the increase of content of Ir complexes in the chelating polymers.

The PL spectra of chelating polymer films (Figure 6) show that when the iridium complex content in the feed ratio was only 0.5 mol%, the blue emission peak became very much less-intense and the red emission peak became dominant. When the content increased to 2 mol%, the blue emission peak almost disappeared, indicating efficient energy transfer from host to guest. The different emission properties of the chelating polymer in dilute solutions and films suggest that with decreasing distance between the host fluorene segments and the guest Ir complexes in film, the energy transfer in the film is more efficient than that in dilute solution.[19]

Figure 8 showed the PL spectra for the blends of charged Ir complex [Ir(Fiq)$_2$(bpy)] doped into PFO. The doping concentration of [Ir(Fiq)$_2$(bpy)] in PFO varied from 0.5 mol% (PFO/[Ir(Fiq)$_2$(bpy)](0.5)), 2 mol% (PFO/[Ir(Fiq)$_2$-(bpy)](2)), 4 mol% (PFO/[Ir(Fiq)$_2$(bpy)](4)), 8 mol% (PFO/[Ir(Fiq)$_2$(bpy)](8)), to 16 mol% (PFO/[Ir(Fiq)$_2$-(bpy)](16)) for comparison. The PL spectra showed that when the doping concentration of charged Ir complex was low, the blue emission band of the host PFO was dominant. Even though the doping concentration was increased to 16 mol%, the host emission was not completely quenched, indicating inefficient energy transfer in the blend system. It

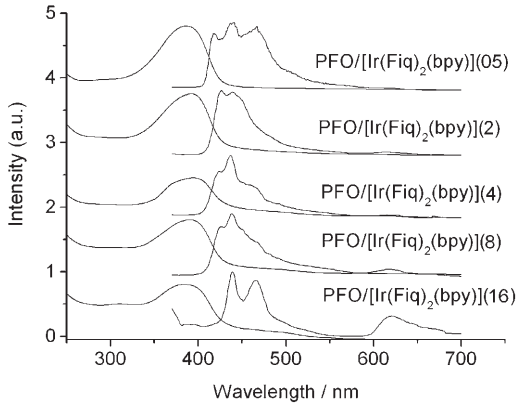

Figure 8. Absorption and PL spectra in films of PFO/[Ir(Fiq)$_2$(bpy)] blends excited at 325 nm.

is worth noting that much more efficient energy transfer can be achieved in the chelating polymers reported in this work, so intramolecular energy transfer might be an efficient process in chelating polymers. A similar phenomenon was reported by Zhen and co-workers[6] During the spin-coating, we found that the quality of the films of the blend system were not good enough because of the poor compatibility of charged Ir complex and hydrophobic conjugated polymer and this may be a reason for the inefficient energy transfer. Consequently, the incorporation of charged Ir complexes into the backbones of conjugated polymers through covalent bonding gives rise to more efficient energy transfer than for the corresponding blended system and the system is also not subject to the intrinsic problems associated with the blends.

The above discussions indicate that in chelating polymers with charged Ir complexes, intra and intermolecular energy transfers coexist and the intramolecular energy transfer may be a more efficient process. This result is consistent with the result reported in chelating polymers with neutral Ir complexes in the conjugated backbone.[6]

It was interesting that the decrease in intensity of three blue emission peaks at about 420 nm, 445 nm, and 472 nm with contributions due to the fluorene segments was very different in the energy-transfer process as shown in Figures 5 and 8b. With the increase of charged Ir complex content in the chelating polymers, the emission peak at about 420 nm underwent the largest decrease in intensity followed by that for the peaks at 445 nm and 472 nm. This may be the result of the different degree of overlap of the blue emission and red absorption spectra of the iridium complex.

The maximum emission peaks of chelating polymers (Table 2) showed a slight red shift with the increase of iridium complex content and all peaks were shifted to the red by less than 10 nm compared with the PL emission of the pristine complex [Ir(Fiq)$_2$(bpy)] in our study, while the PL emissions from [Ir(Fiq)$_2$(bpy)] in the doped systems were almost identical with that of [Ir(Fiq)$_2$(bpy)]. A similar phenomenon was observed in the previous study,[6] in which the PL emission bands of chelating polymers shifted to the red by around 50–60 nm, a much larger shift than that in our study. The reason for the red shift may be explained as the result of the extended conjugation length of the ligand. The slight red shift in our study may be due to the poor coplanarity of the bipyridine and the neighboring fluorene segments in the chelating polymers, so that there is not much change in the conjugation length of the ligand.

Transient luminescent decays monitored at $\lambda = 445$ nm due to the peak emission of the host PFO and the chelating polymers were measured to further study the energy migration. For PFO, single exponential decay with a fluorescence lifetime τ of 2.4 ns was observed. However, the fluorescent lifetimes recorded at 445 nm were 1.88 and 1.65 ns for PFO-Ir05 and PFO-Ir2 respectively, and those of PFO-Ir4, PFO-Ir8, and PFO-Ir16 could not be measured due to the weak counts. The study of Gong and co-workers[20] showed that the decay time of the fluorescence associated with a PFO film with a higher concentration of Ir complexes was much shorter than that for films with lower concentration, indicating that energy transfer in the former was more efficient than that in the latter. Therefore the observation that the fluorescence decay time monitored at 445 nm for PFO-Ir05 is much shorter than that for PFO and becomes even shorter when the concentration of guest-charged Ir complex increases to 2 mol% proving that the energy migration does occur from the host fluorene segments to the guest-charged Ir complex units as mentioned above. A higher content of charged Ir complexes in the backbones of the polymer will induce more-efficient energy transfer from host to guest. Moreover, for these chelating polymers, the observed lifetimes recorded at around 625 nm were 0.52–1.51 μs in films indicating the triplet nature of the long-wavelength emission band, and the lifetimes became shorter with the increase of iridium-complex content due to the quenching associated with molecular packing. The luminescent decay times are summarized in Table 2.

The absolute PL efficiency measurement of the chelating polymer films was measured in an integrating sphere excited at 325 nm. Introducing Ir complex into the polymer main chains reduced PL efficiency (Table 2). Therefore, PL quantum efficiencies Φ_{PL} had been moderated, and the Φ_{PL} decreased slightly with the increase of Ir-complex content because of T–T annihilation and/or concentration quenching.[21]

Electrochemical properties: The redox properties of the charged Ir complex and chelating polymers were investigated by cyclic voltammetry (CV). All chelating polymers exhibited good reversibility with onset around 0.92 ~ 0.96 V and −2.59 ~ −2.65 V against an Ag/AgNO$_3$ reference electrode for the oxidation and reduction process, respectively (Figure 9). According to the redox onset potentials of the CV measurements, the HOMO/LUMO energy levels of the materials were estimated based on the reference energy level of ferrocene (4.8 eV below the vacuum): HOMO/LUMO $= -(E_{onset} - (-0.04\ V)) - 4.8$ eV,[22] where the value −0.04 V was for ferrocene/ferrocenium (FOC) versus Ag/Ag$^+$. As shown in Table 3, HOMO levels of all chelating

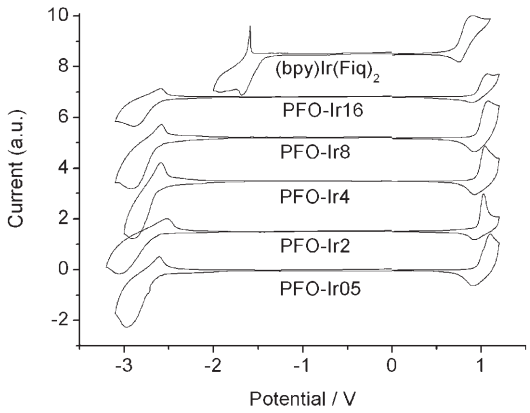

Figure 9. Cyclic voltammograms of $[Ir(Fiq)_2(bpy)]$ and chelating polymer films.

Table 3. Electrochemical properties of the copolymers and $[Ir(Fiq)_2(bpy)]$.

Polymer	*n*-doping [V][a]			*p*-doping [V][a]			energy levels [eV]		
	E_{onset}	E_{pc}	E_{pa}	E_{onset}	E_{pa}	E_{pc}	HOMO	LUMO	E_g[b]
PFO-Ir05	−2.65	−2.98	−2.61	0.96	1.10	0.91	−5.80	−2.19	3.61
PFO-Ir2	−2.64	−3.06	−2.52	0.96	1.03	0.92	−5.80	−2.20	3.60
PFO-Ir4	−2.62	−2.91	−2.59	0.94	1.04	0.92	−5.78	−2.22	3.56
PFO-Ir8	−2.61	−2.92	−2.58	0.93	1.07	0.92	−5.77	−2.23	3.54
PFO-Ir16	−2.59	−2.89	−2.59	0.92	1.07	0.89	−5.76	−2.25	3.51
$[Ir(Fiq)_2(bpy)]$	−1.43	−1.70	−1.60	0.69	0.90	0.75	−5.53	−3.39	2.41

[a] E_{pa} and E_{pc} stand for anodic peak potential and cathodic peak potential, respectively. [b] E_g stands for the band-gap energy.

polymers were estimated at about −5.76 ~ −5.80 eV, and LUMO levels at about −2.19 ~ −2.25 eV. It was reported that the HOMO and LUMO energy levels of PFO measured by the electrochemical method were −5.8 and −2.12 eV.[23] Comparing our results with those of the references, we found that the chelating polymers have almost the same HOMO energy level as that of PFO, but the LUMO energy level is slightly lower than that of PFO suggesting that the chelating polymers reported in this work have better electron injection and transporting properties due to the incorporation of charged Ir complexes into the main chain of the polymer. The oxidation and reduction potentials for $[Ir(Fiq)_2(bpy)]$ were observed at 0.69 and −1.43 V, respectively. Therefore the HOMO and LUMO level were at −5.53 and −3.39 eV, respectively. If the HOMO and LUMO level of the charged Ir complex, which was chelated into the main chains of the polymer do not change, they would fall within the band gap of the host fluorene segments. As a result, the charged Ir complex chelated into the backbone of the polymer would function as both a hole and an electron trap.[24] The good redox reversibility not only allows us to study the electronic properties of the chelating polymers but also proves that they may be good candidates as electrophosphorescent materials for applications in polymer light-emitting diodes.

Conclusion

We successfully designed and synthesized a series of π-conjugated chelating polymers that emit red light by the copolymerization of the fluorene unit and the charged Ir complex unit. The energy transfer, thermal stability, photophysical, and electrochemical properties have been investigated in detail. Almost complete energy transfer from the host fluorene segments to the guest Ir complexes was achieved in the solid state when the feed ratio was 2 mol%. However in the corresponding blend system, energy transfer was not complete even when the content of Ir complexes was as high as 16 mol%. Intra- and inter-chain energy transfer mechanisms coexisted in the energy-migration process of this host–guest system, and the intramolecular energy transfer might be a more efficient process. The chelating polymers showed more-efficient energy transfer than the corresponding blended system and also exhibited good thermal stability, redox reversibility, and film formation. Therefore, they may be good candidates for many applications, such as LECs and polymer electroluminescent materials in light-emitting diodes. The fabrication of devices by using these copolymers as light-emitting layers, and the factors influencing the performance of such devices are under investigation.

Experimental Section

Measurements: UV/Vis absorption spectra were recorded by using a Shimadzu 3000 UV-visible-NIR spectrophotometer. NMR spectra were recorded on a Mercury Plus 400 MHz NMR spectrometer. The elemental analyses were performed on a Vario EL III O-Element Analyzer system. Mass spectra were obtained on a Shimadzu laser desorption/ionization time-of-flight mass spectrometer (LDI-TOF-MASS). The photoluminescence spectra were measured on an Edinburgh LFS920 fluorescence spectrophotometer. Fluorescence lifetimes were recorded on a single-photon-counting spectrometer from Edinburgh Instruments (FLS920) with a hydrogen-filled pulse lamp as the excitation source. The data were analyzed by iterative convolutions of the luminescence decay profile with the instrument response function by using the software package provided by Edinburgh Instruments. Thermogravimetric analysis (TGA) and differential scanning calorimetry (DSC) were performed on Shimadzu DSC-60 A and DTG-60 A thermal analyzers under nitrogen atmosphere at a heating rate of 10 °C min^{-1}. CV was performed on an Eco Chemie Autolab instrument by coating the film on working electrodes in a solution of Bu_4NPF_6 (0.10 M) in acetonitrile at a scan rate of 100 mV s^{-1} at room temperature. CV was conducted at room temperature in a typical three-electrode cell with a working electrode (glassy carbon electrode), a reference electrode (Ag/Ag^+, referenced against ferrocene/ferrocenium (FOC)), and a counter electrode (Pt wire) under a nitrogen atmosphere at a sweeping rate of 100 mV s^{-1}. The onset potentials were determined from the intersection of two tangents drawn at the rising current and background current of the cyclic voltammogram. The GPC analysis of the polymers was conducted on a Shimadzu 10 A with THF as the eluent

and poly(styrene) as standard. The data were analyzed by using the software package provided by Shimadzu Instruments. Measurement of the absolute PL efficiency was performed on a Labsphere IS-080 (8″) instrument, which contained an integrating sphere coated on the inside with a reflecting material barium sulfate, and the diameter of the integrating sphere was 8 inches. PL efficiency was calculated by using the LabsphereIS-080 (8″) software.

Materials: All manipulations involving air-sensitive reagents were performed in an atmosphere of dry N_2 gas. The solvents (THF, toluene) were purified by routine procedures and distilled under dry N_2 before use. All reagents, unless otherwise specified, were purchased from Aldrich, Acros, and Lancaster and were used as received.

2-Bromo-9,9-dioctylfluorene (1): 1-Bromooctane (8.5 g, 44.0 mmol) was added by using a syringe to a mixture of 2-bromofluorene (4.5 g, 20.0 mmol) and KOH (11.2 g, 200.0 mmol) in DMSO (10 mL). The solution was stirred at 60 °C overnight. The mixture was poured into H_2O (200 mL), and then was extracted three times with ethyl acetate. The combined organic layers were washed with brine and dried over anhydrous $MgSO_4$. The solvent was removed under reduced pressure. The crude product was purified by column chromatography by using hexane as eluent to yield a colorless oil (8.8 g, 94 %). ^{1}H NMR (400 MHz, $CDCl_3$): δ = 7.65 (m, 1H), 7.54 (m, 1H), 7.44 (m, 2H), 7.31 (m, 3H), 1.92 (m, 4H), 0.97–1.24 (m, 20H), 0.81 (t, J = 7.2 Hz, 6H), 0.58 ppm (m, 4H); elemental analysis calcd (%) for $C_{29}H_{41}Br$: C 74.18, H 8.80; found: C 74.48, H 8.82.

9,9-Dioctylfluorene-2-boronic acid (2): *n*-Butyllithium in hexane (1.6 M, 14.6 mL, 23.4 mmol) was added dropwise to a solution of compound **1** (10.0 g, 21.3 mmol) in THF (80 mL) at −78 °C. After 45 min, trimethyl boronate (5.5 g, 53.3 mmol) was added by syringe. Then the mixture was allowed to warm to room temperature slowly and was stirred overnight. HCl (2 N, 100 mL) was added to the stirred solution while maintaining the solution at 0 °C for 1 h. The organic layer was separated and the water layer was extracted with diethyl ether (150 mL). The combined ether layers were washed twice with brine (100 mL) and were then dried over anhydrous $MgSO_4$. The solvent was removed under reduced pressure. The crude product was purified by column chromatography by using hexane and ethyl acetate (3:1 v/v) as eluent to yield a white solid (6.8 g, 73 %). ^{1}H NMR (400 MHz, $CDCl_3$): δ = 8.31 (m, 1H), 8.22 (s, 1H), 7.89 (d, J = 7.2 Hz, 1H), 7.81 (m, 1H), 7.38 (m, 3H), 2.09 (m, 4H), 0.97–1.22 (m, 20H), 0.77 (t, J = 7.2 Hz, 6H), 0.68 ppm (m, 4H); elemental analysis calcd (%) for $C_{29}H_{43}O_2B$: C 80.17, H 9.98; found: C 80.04, H 9.75.

1-(9,9-Dioctylfluorene-2-yl)isoquinoline (Fiq) (3): Tetrakis(triphenylphosphine)palladium (0.4 g, 0.4 mmol) was added to a mixture of 1-chloroisoquinoline (1.9 g, 11.5 mmol), compound **2** (5.0 g, 11.5 mmol), toluene (50 mL), ethanol (25 mL), and 2 M sodium carbonate aqueous solution (25 mL) with vigorous stirring. The mixture was stirred at 70 °C for 24 h under N_2 atmosphere. After cooling to room temperature, the mixture was poured into water and then was extracted with ethyl acetate. The organic layer was washed with brine several times. Then, the solvent was evaporated. The product thus obtained was purified by silica-gel column chromatography by using hexane and ethyl acetate (9:1 v/v) as eluent to yield a colorless oil (5.0 g, 83 %). ^{1}H NMR (400 MHz, $CDCl_3$): δ = 8.65 (d, J = 5.6 Hz, 1H), 8.10 (d, J = 8.8 Hz, 1H), 7.85–7.92 (m, 2H), 7.78 (m, 1H), 7.64–7.73 (m, 4H), 7.52 (m, 1H), 7.30–7.40 (m, 3H), 2.01 (m, 4H), 1.02–1.21 (m, 20H), 0.80 (t, 6H), 0.72 ppm (m, 4H); elemental analysis calcd (%) for $C_{38}H_{47}N$: C 88.15, H 9.15, N 2.71; found: C 88.41, H 9.20, N 2.57.

5,5′-Dibromo-2,2′-bipyridine (4): Compound **4** was synthesized according to reference [25] but the yield obtained in our work was lower than that reported. To the mixture of 2,5-dibromopyridine (2.0 g, 8.7 mmol) and $[Pd(PPh_3)_4]$ (0.2 g, 0.2 mmol) in a flask, anhydrous and degassed *m*-xylene (70 mL) was added from a syringe, followed by hexa-*n*-butyldistannane (2.46 mL) under N_2 atmosphere. The mixture was heated at 130 °C for three days until all starting material was consumed and was then poured into aqueous EDTA (0.2 M, 250 mL). After the mixture was stirred for 30 min, the phases were separated. The aqueous phase was extracted with chloroform (3 × 100 mL), and the combined organic phases were dried over Na_2SO_4. After evaporation of the solvents, the crude product was recrystallized from CH_2Cl_2 to give white acerose crystals (0.98 g, 65 %). ^{1}H NMR (400 MHz, $CDCl_3$): δ = 7.91 (dd, J = 8.4, J = 2.4 Hz, 2H), 8.26 (d, J = 8.4 Hz, 2H), 8.68 ppm (d, J = 2 Hz, 2H).

[Ir(Fiq)$_2$(BrbpyBr)] (M3): Cyclometalated Ir^{III} μ-chloro-bridged dimer **5** was synthesized by the method reported by Nonoyama.[26] $IrCl_3 \cdot 3H_2O$ (2.0 g, 5.5 mmol) and **3** (5.7 g, 11.0 mmol) were heated in a 3:1 mixture of 2-ethoxyethanol and water (40 mL) under N_2 atmosphere. The slurry was heated at 110 °C for 24 h. After the mixture had been cooled to room temperature, the precipitate was filtered off and washed with water and ethanol to obtain red solid **5**. CH_2Cl_2 and methanol (30 mL, 2:1 v/v) were added to the mixture of **5** (0.4 g, 0.2 mmol) and **4** (0.1 g, 0.3 mmol) under N_2 atmosphere. The mixture was refluxed for 4 h, then cooled to room temperature, before fivefold KPF_6 was added and the mixture was stirred for 1 h. The solvent was removed and the solid was dissolved again in CH_2Cl_2 (20 mL), the precipitate was filtered off and methanol was layered onto the filtrate. Red crystals of [Ir(Fiq)$_2$(BrbpyBr)] could be recrystallized from the solution (6.5 g, 70 %). ^{1}H NMR (400 MHz, [D$_6$]DMSO): δ = 8.94 (m, 4H), 8.60 (m, 2H), 8.17–8.31 (m, 4H), 7.57–7.96 (m, 10H), 7.22–7.34 (m, 4H), 7.11 (m, J = 7.6 Hz, 2H), 6.78 (d, J = 7.6 Hz, 2H), 6.46 (s, 2H), 2.12 (m, 8H), 0.75–1.08 (m, 40H), 0.37–0.71 ppm (m, 20H); ^{13}C NMR (100 MHz, $CDCl_3$): δ = 169.67, 154.16, 152.40, 151.48, 151.25, 145.36, 144.28, 144.11, 142.73, 140.78, 139.91, 137.47, 132.20, 129.10, 128.26, 128.00, 127.50, 126.95, 126.87, 126.52, 125.48, 125.17, 123.12, 123.07, 121.98, 120.48, 54.91, 41.17, 40.05, 32.10, 32.01, 30.33, 30.28, 29.61, 29.51, 29.42, 24.48, 23.79, 22.85, 22.82, 14.34, 14.30 ppm; elemental analysis calcd (%) for $C_{86}H_{98}Br_2F_6IrN_4P$: C 61.31, H 5.86, N 3.33; found: C 61.20, H 5.99, N 3.34; MALDI-TOF MS: m/z: [$M-PF_6^-$]: 1539.8; found: 1539.8.

[Ir(Fiq)$_2$(bpy)] (6): Yield 71 %. The synthesis method is similar to that for **M3**. ^{1}H NMR (400 MHz, $CDCl_3$): δ = 8.78–8.93 (m, 4H), 7.81–8.18 (m, 10H), 7.62 (m, 2H), 7.09–7.40 (m, 12H), 6.97 (d, J = 7.6 Hz, 2H), 6.61 (s, 2H), 2.00 (m, 8H), 1.04–1.15 (m, 40H), 0.58–0.90 ppm (m, 20H); elemental analysis calcd (%) for $C_{86}H_{100}F_6IrN_4P$: C 67.65, H 6.60, N 3.67; found: C 67.61, H 6.58, N 3.68.

9,9-Dioctylfluorene (7): 1-Bromooctane (21.3 g, 110 mmol) was added using a syringe to a mixture of fluorene (8.3 g, 50.0 mmol) and KOH (28 g, 500 mmol) in THF (120 mL) at room temperature. After workup, the mixture was poured into water and extracted with ethyl acetate. The organic extracts were washed with brine and dried over magnesium sulfate. The solvent was removed under reduced pressure. The crude product was purified by column chromatography by using hexane as eluent to give a yellow oil (17.58 g, 85 %). ^{1}H NMR (400 MHz, $CDCl_3$): δ = 7.83 (dd, J = 4.3 Hz, 2H), 7.43 (m, 6H), 2.12 (m, 4H), 1.35–1.24 (m, 20H), 0.96 (t, J = 7.1 Hz, 6H), 0.79 ppm (m, 4H).

9,9-Dioctyl-2,7-dibromofluorene (M2): Ferric chloride (75 mg, 0.5 mmol) and bromine (3.2 mL, 63.0 mmol) were added to a solution of 9,9-dioctylfluorene (11.7 g, 30 mmol) in $CHCl_3$ (50 mL) at 0 °C. The reaction proceeded in the dark. The solution was warmed to room temperature and was stirred for 3 h. The resulting slurry was poured into water and was washed with sodium thiosulfate solution until the red color disappeared. The aqueous layer was extracted with ethyl acetate (three times), and the combined organic layers were dried over magnesium sulfate to afford 9,9-dioctyl-2,7-dibromofluorene (15.5 g, 94 %) as a yellow solid. The crude product was recrystallized from ethanol. ^{1}H NMR (400 MHz, $CDCl_3$): δ = 7.51 (d, J = 8.8 Hz, 2H), 7.46 (d, J = 1.6 Hz, 2H), 7.44 (s, 2H), 1.91 (m, 4H), 1.99–1.22 (m, 20H), 0.83 (t, J = 7.2 Hz, 6H), 0.57 ppm (m, 4H); ^{13}C NMR (100 MHz, $CDCl_3$): δ = 152.31, 139.97, 130.04, 126.07, 121.38, 120.96, 55.56, 40.02, 31.63, 29.78, 29.04, 29.01, 23.51, 22.47, 13.94 ppm; elemental analysis calcd (%) for $C_{29}H_{40}Br_2$: C 63.51, H 7.35; found: C 63.64, H 7.53.

9,9-Dioctylfluorene-2,7-bis(trimethylene boronate) (M1): A solution of 2,7-dibromo-9,9-dioctylfluorene (11.0 g, 20.0 mmol) in dry THF was added slowly to a stirred mixture of magnesium turnings (1.2 g, 50.0 mmol) in dry THF containing a catalytic amount of iodine under nitrogen to form the Grignard reagent. The Grignard reagent solution was slowly dropped into a stirred solution of trimethyl borate (11.5 mL, 100 mmol) in dry THF at −78 °C over a period of 1.5 h and was then

slowly warmed to room temperature. The mixture was stirred (vigorous stirring was required to avoid gel formation) at room temperature for three days and then was poured onto a mixture of crushed ice containing sulfuric acid (5%) with stirring. The mixture was extracted with ether, and the combined extracts were evaporated to give 9,9-dioctylfluorene-2,7-diboronic acid. The crude acid was washed with hexane to give a white solid (4.3 g, 45%). The diboronic acid was then refluxed with 1,3-propanediol (1.2 g, 20 mmol) in toluene for 10 h. After working up, the crude product was recrystallized from hexane to afford 9,9-dioctylfluorene-2,7-bis-(trimethylene boronate) (3.6 g, 72%) as white crystals. ^{1}H NMR (400 MHz, $CDCl_3$): $\delta = 7.75$ (d, $J = 8.4$ Hz, 2H), 7.67–7.72 (m, 4H), 4.21 (t, 8H), 2.10 (m, 4H), 1.98 (m, 4H), 0.92–1.23 (m, 20H), 0.81 (t, $J = 7.2$ Hz, 6H), 0.52 ppm (m, 4H); elemental analysis calcd (%) for $C_{35}H_{52}B_2O_4$: C 75.28, H 9.39; found: C 75.45, H 9.75.

General procedure for the copolymerization of fluorene and Ir complex by the Suzuki cross coupling method: To a mixture of 9,9-dioctylfluorene-2,7-bis(trimethylene boronate) (1 equiv), dibromo compound (1 equiv), including the Ir complex and 9,9-dioctyl-2,7-dibromofluorene, tetrabutylammonium bromide, and 4.0 mol% [$Pd(PPh_3)_4$], was added a degassed mixture of toluene ([monomer] = 0.25 M) and aqueous 2 M potassium carbonate (3:2 in volume). The mixture was vigorously stirred at 85–90 °C for 72 h and then bromobenzene was added. After the mixture was cooled to room temperature, it was washed with water. The solution was concentrated and then it was slowly add dropwise to a mixture of methanol and deionized water (220 mL, 10:1 v/v). A fibrous solid was obtained by filtration. The solid was dissolved in THF and then the solution was evaporated. The concentrated solution obtained was dropped slowly into methanol (250 mL) again. And this procedure was repeated twice in acetone in place of methanol. The fibrous solid was filtered and was then washed with acetone in a Soxhlet apparatus for 3–5 days to remove oligomers and catalyst residues. The resulting polymers were collected and dried under vacuum. Yields: 55–70%.

PFO: ^{1}H NMR (400 MHz, $CDCl_3$): $\delta = 7.66$–7.86 (m, 6H), 2.12 (m, 4H), 1.05–1.28 (m, 20H), 0.63–0.89 ppm (m, 10H); ^{13}C NMR (100 MHz, $CDCl_3$): $\delta = 151.81$, 140.68, 140.02, 126.18, 121.49, 120.22, 55.34, 40.43, 31.93, 30.88, 30.08, 29.37, 24.12, 22.64, 14.28 ppm; elemental analysis calcd (%): C 89.62, H 10.38; found: C 88.86, H 10.07.

PFO-Ir05: ^{1}H NMR (400 MHz, $CDCl_3$): $\delta = 7.67$–7.85 (m, 6H), 2.12 (m, 4H), 1.05–1.28 (m, 20H), 0.63–0.89 ppm (m, 10H); ^{13}C NMR (100 MHz, $CDCl_3$): $\delta = 152.04$, 140.72, 140.26, 126.39, 121.72, 120.21, 55.57, 40.62, 32.03, 30.28, 30.18, 29.46, 24.14, 22.84, 14.31 ppm; elemental analysis calcd (%): C 87.96, H 10.22, N 0.07; found: C 84.52, H 9.73, N 0.21.

PFO-Ir2: ^{1}H NMR (400 MHz, $CDCl_3$): $\delta = 7.67$–7.85 (m, 6H), 2.12 (m, 4H), 1.05–1.28 (m, 20H), 0.63–0.89 ppm (m, 10H); ^{13}C NMR (100 MHz, $CDCl_3$): $\delta = 151.81$, 140.50, 140.02, 128.79, 127.21, 126.17, 121.49, 119.98, 55.34, 40.38, 31.80, 30.96, 30.04, 29.23, 23.92, 22.61, 14.08 ppm; elemental analysis calcd (%): C 88.05, H 10.03, N 0.27; found: C 86.61, H 10.03, N 0.23.

PFO-Ir4: ^{1}H NMR (400 MHz, $CDCl_3$): $\delta = 7.67$–7.85 (m, 6H), 2.12 (m, 4H), 0.95–1.38 (m, 20H), 0.59–0.82 (m, 10H), 9.02 (m, 3.6% × 4H; Ar*H* of Ir complex), 8.30 (m, 3.6% × 4H; Ar*H* of Ir complex), 7.10 (m, 3.6% × 2H; Ar*H* of Ir complex), 6.85 ppm (m, 3.6% × 2H; Ar*H* of Ir complex); ^{13}C NMR (100 MHz, $CDCl_3$): $\delta = 152.05$, 140.72, 140.25, 129.03, 127.45, 126.40, 121.72, 120.22, 55.60, 40.63, 32.04, 31.21, 30.28, 29.48, 24.15, 22.85, 14.33 ppm; elemental analysis calcd (%): C 86.83, H 9.88, N 0.47; found: C 85.47, H 10.01, N 0.43. According to the NMR data, the Ir complex content in the copolymer was around 3.6%.

PFO-Ir8: ^{1}H NMR (400 MHz, $CDCl_3$): $\delta = 7.67$–7.85 (m, 6H), 2.12 (m, 4H), 0.95–1.36 (m, 20H), 0.60–0.85 (m, 10H), 9.02 (m, 5.5% × 4H; Ar*H* of Ir complex), 8.30 (m, 5.5% × 4H; Ar*H* of Ir complex), 7.10 (m, 5.5% × 2H; Ar*H* of Ir complex), 6.86 ppm (m, 5.5% × 2H; Ar*H* of Ir complex); ^{13}C NMR (100 MHz, $CDCl_3$): $\delta = 152.04$, 140.72, 140.25, 129.03, 127.44, 126.39, 121.72, 120.21, 55.57, 40.63, 32.03, 31.19, 30.27, 29.46, 24.14, 22.84, 14.32 ppm; elemental analysis calcd (%): C 86.50, H 9.76, N 0.70; found: C 84.54, H 9.87, N 0.60. According to the NMR data, the Ir complex content in the copolymer was around 5.5%.

PFO-Ir16: ^{1}H NMR (400 MHz, $CDCl_3$): $\delta = 7.67$–7.85 (m, 6H), 2.12 (m, 4H), 0.95–1.36 (m, 20H), 0.63–0.86 (m, 10H), 9.02 (m, 11% × 4H; Ar*H* of Ir complex), 8.30 (m, 11% × 4H; Ar*H* of Ir complex), 7.10 (m, 11% × 2H; Ar*H* of Ir complex), 6.86 ppm (m, 11% × 2H; Ar*H* of Ir complex); ^{13}C NMR (100 MHz, $CDCl_3$): $\delta = 152.04$, 140.72, 140.24, 129.03, 127.44, 126.39, 121.72, 120.21, 55.57, 40.63, 32.04, 31.20, 30.27, 29.46, 24.14, 22.85, 14.32 ppm; elemental analysis calcd (%): C 82.47, H 9.10, N 1.20; found: C 79.37, H 8.86, N 1.24. According to the NMR data, the Ir complex content in the copolymer was around 11%.

Acknowledgements

This work was financially supported by the National Natural Science Foundation of China under Grants 60325412, 90406021, 50428303, and 20504007 as well as the Shanghai Commission of Science and Technology under Grants 03DZ11016, and 04XD14002, and the Shanghai Commission of Education under Grant 2003SG03.

[1] a) M. A. Baldo, D. F. O'Brien, Y. You, A. Shoustikov, S. Sibley, M. E. Thompson, S. R. Forrest, *Nature* **1998**, *395*, 151–154; b) S. Lamansky, R. C. Kwong, M. Nugent, P. I. Djurovich, M. E. Thompson, *Org. Electron.* **2001**, *2*, 53–62; c) X. Gong, M. R. Robinson, J. C. Ostrowski, D. Moses, G. C. Bazan, A. J. Heeger, *Adv. Mater.* **2002**, *14*, 581–585.

[2] a) E. Holder, B. M. W. Langeveld, U. S. Schubert. *Adv. Mater.* **2005**, *17*, 1109–1121; b) T. D. Anthopoulos, M. J. Frampton, E. B. Namdas, P. L. Burn, I. D. W. Samuel. *Adv. Mater.* **2004**, *16*, 557–560; c) C. Adachi, M. A. Baldo, M. E. Thompson, S. R. Forrest, *J. Appl. Phys.* **2001**, *90*, 5048–5051; d) E. Tekin, E. Holder, V. Marin, B.-J. de Gans, U. S. Schubert, *Macromol. Rapid Commun.* **2005**, *26*, 293–297; e) E. Holder, V. Marin, D. Kozodaev, M. A. R. Meier, B. G. G. Lohmeijer, U. S. Schubert, *Macromol. Chem. Phys.* **2005**, *206*, 989–997.

[3] a) J. H. Burroughes, D. D. C. Bradley, A. R. Brown, R. N. Marks, K. Mackay, R. H. Friend, P. L. Burns, A. B. Holmes, *Nature* **1990**, *347*, 539–541; b) C. Adachi, M. A. Baldo, S. R. Forrest, S. Lamansky, M. E. Thompson, R. C. Kwong, *Appl. Phys. Lett.* **2001**, *78*, 1622–1624; c) G. E. Jabbour, J. F. Wang, N. Peyghambarian, *Appl. Phys. Lett.* **2002**, *80*, 2026–2028; d) J. P. Duan, P. P. Sun, C. H. Cheng, *Adv. Mater.* **2003**, *15*, 224–228; e) S. Lamansky, P. Djurovich, D. Murphy, F. Abdel-Razzaq, H.-E. Lee, C. Adachi, P. E. Burrows, S. R. Forrest, M. E. Thompson, *J. Am. Chem. Soc.* **2001**, *123*, 4304–4312.

[4] a) M. A. Baldo, S. Lamansky, P. E. Burrows, M. E. Thompson, S. R. Forrest, *Appl. Phys. Lett.* **1999**, *75*, 4–6; b) M. J. Frampton, E. B. Namdas, S.-C. Lo, P. L. Burn, I. D. W. Samuel, *J. Mater. Chem.* **2004**, *14*, 2881–2888.

[5] a) K. M. Vaeth, C. W. Tang, *J. Appl. Phys.* **2002**, *92*, 3447–3453; b) A. Dijken, J. J. A. M. Bastiaansen, N. M. M. Kiggen, B. M. W. Langeveld, C. Rothe, A. Monkman, I. Bach, P. Stössel, K. Brunner, *J. Am. Chem. Soc.* **2004**, *126*, 7718–7727; c) K. Brunner, A. Dijken, H. Börner, J. J. A. M. Bastiaansen, N. M. M. Kiggen, B. M. W. Langeveld, *J. Am. Chem. Soc.* **2004**, *126*, 6035–6042; d) C. Y. Jiang, W. Yang, J. B. Peng, S. Xiao, Y. Cao, *Adv. Mater.* **2004**, *16*, 537–541.

[6] a) H. Y. Zhen, C. Y. Jiang, W. Yang, J. X. Jiang, F. Huang, Y. Cao, *Chem. Eur. J.* **2005**, *11*, 5007–5016; b) Z. Wang, A. R. McWilliams, C. E. B. Evans, X. Lu, S. Chung, M. A. Winnik, I. Manners, *Adv. Funct. Mater.* **2002**, *12*, 415–419.

[7] X. Chen, J.-L. Liao, Y. Liang, M. O. Ahmed, H.-E. Tseng, S.-A. Chen, *J. Am. Chem. Soc.* **2003**, *125*, 636–637.

[8] A. J. Sandee, C. K. Williams, N. R. Evans, J. E. Davies, C. E. Boothby, A. Köhler, R. H. Friend, A. B. Holmes, *J. Am. Chem. Soc.* **2004**, *126*, 7041–7048.

[9] J. X. Jiang, C. Y. Jiang, W. Yang, H. Y. Zhen, F. Huang, Y. Cao, *Macromolecules* **2005**, *38*, 4072–4080.

[10] a) C. L. Lee, N. G. Kang, Y. S. Cho, J. S. Lee, J. J. Kim, *Opt. Mater.* **2002**, 21, 119–123; b) S. Tokito, M. Suzuki, F. Sato, M. Kamachi, K. Shirane, *Org. Electron.* **2003**, *4*, 105–111; c) X. D. Wang, K. Ogino,

K. Tanaka, H. Usui, *IEEE J. Sel. Top. Quantum Electron.* **2004**, *10*, 121–126.
[11] a) E. A. Phummer, A. Dijken, H. W. Hofstraat, L. D. Cola, K. Brunner, *Adv. Funct. Mater.* **2005**, *15*, 281–289; b) J. D. Slinker, A. A. Gorodetsky, M. S. Lowry, J. Wang, S. Parker, R. Rohl, S. Bernhard, G. G. Malliaras, *J. Am. Chem. Soc.* **2004**, *126*, 2763–2767.
[12] a) E. Holder, V. Marin, M. A. R. Meier, U. S. Schubert, *Macromol. Rapid Commun.* **2004**, *25*, 1491–1496; b) V. Marin, E. Holder, R. Hoogenboom, U. S. Schubert, *J. Polym. Sci. Part A: Polym. Chem.* **2004**, *42*, 4153–4160.
[13] B. Liu, W.-L. Yu, Y.-H. Lai, W. Huang, *Macromolecules* **2002**, *35*, 4975–4982.
[14] R. Fink, Y. Heischkel, M. Thelakkat, H. Schmidt, *Chem. Mater.* **1998**, *10*, 3620–3625.
[15] B. Liu, W. Huang, *Thin Solid Films* **2002**, *417*, 206–210.
[16] B. Liu, W.-L. Yu, Y.-H. Lai, W. Huang, *Chem. Mater.* **2001**, *13*, 1984–1991.
[17] M. A. Baldo, M. E. Thompson, S. R. Forrest, *Nature* **2000**, *403*, 750–753.
[18] a) T. Föster, *Discuss. Faraday Soc.* **1959**, *27*, 7–17; b) D. L. Dexter, *J. Chem. Phys.* **1953**, *21*, 836–850.
[19] X. Gong, J. C. Ostrowski, D. Moses, G. C. Bazan, A. J. Heeger, *Adv. Funct. Mater.* **2003**, *13*, 439–444.
[20] X. Gong, S.-H. Lim, J. C. Ostrowski, D. Moses, C. J. Bardeen, G. C. Bazan, *J. Appl. Phys.* **2004**, 95, 948–953.
[21] M. Zhang, P. Lu, X. M. Wang, L. He, H. Xia, W. Zhang, B. Yang, L. L. Liu, L. Yang, M. Yang, Y. G. Ma, J. K. Feng, D. J. Wang, N. Tamai, *J. Phys. Chem. B* **2004**, *108*, 13185–13190.
[22] M. S. Liu, J. D. Luo, A. K-Y. Jen, *Chem. Mater.* **2003**, *15*, 3496–3500.
[23] S. Janietz, D. D. C. Bradley, M. Grell, C. Giebeler, M. Inbasekaran, E. P. Woo, *Appl. Phys. Lett.* **1998**, 73, 2453–2455.
[24] X. H. Yang, D. Neher, D. Hertel, T. H. Daubler, *Adv. Mater.* **2004**, *16*, 161–166.
[25] a) P. F. H. Schwab, F. Fleischer, J. Michl, *J. Org. Chem.* **2002**, *67*, 443–449; b) G. R. Newkome, A. K. Patri, E. Holder, U. S. Schubert, *Eur. J. Org. Chem.* **2004**, 235–254.
[26] K. Nonoyama, *Bull. Chem. Soc. Jpn*, **1974**, *47*, 467

Received: September 5, 2005
Revised: January 12, 2006
Published online: March 20, 2006

